

G. 55.



ИНСТИТУТ ЯДЕРНОЙ ФИЗИКИ СО АН СССР

E.S.Gluskin, P.P.Ilyinsky, G.Ya.Kezerashvili,  
G.N.Kulipanov, V.V.Pindyurin, A.N.Skrinsky,  
A.S.Sokolov

THE STUDY OF THE RADIATION FROM  
THE HELICAL UNDULATOR INSTALLED IN  
THE STORAGE RING VEPP-2M AS A SOURCE  
FOR X-RAY MICROSCOPY AND HOLOGRAPHY

PREPRINT 83-145

БИБЛИОТЕКА  
Института ядерной  
Физики СО АН СССР  
ИНВ. № \_\_\_\_\_



НОВОСИБИРСК

Institute of Nuclear Physics

E.S.Gluskin, P.P.Ilyinsky, G.Ya.Kezerashvili,  
G.N.Kulipanov, V.V.Pindyurin, A.N.Skrinsky,  
A.S.Sokolov

THE STUDY OF THE RADIATION FROM THE HELICAL  
UNDULATOR INSTALLED IN THE STORAGE RING  
VEPP-2M AS A SOURCE FOR X-RAY MICROSCOPY  
AND HOLOGRAPHY

Preprint

Novosibirsk

THE STUDY OF THE RADIATION FROM THE HELICAL  
UNDULATOR INSTALLED IN THE STORAGE RING  
VEPP-2M AS A SOURCE FOR X-RAY MICROSCOPY  
AND HOLOGRAPHY

E.S.Gluskin, G.Ya.Kezerashvili, G.N.Kulipanov,  
V.F.Pindyurin, A.N.Skrinsky, A.S.Sokolov

Institute of Nuclear Physics,  
630090, Novosibirsk 90, USSR

P.P.Ilyinsky  
Novosibirsk State University

A b s t r a c t

In the work presented here the possibilities of using the undulator radiation (UR) in the holographic microscopy are considered. The absolute measurements of the spectral-angular density of UR and the experiments on observation of the UR spatial coherence have been performed aiming to the study of the undulator real parameters.

The development of various techniques of X-ray microscopy was stimulated with an advent of powerful sources of synchrotron radiation (SR). The most impressive results are obtained in the field of a contact microscopy /1/, and a scanning microscopy /2/. The microscopy using the elements of the X-ray optics: the Fresnel zone plates /3,4/, the multi-layer interference mirrors /5/ is in a good progress. In recent years there are many discussions /6,7/ devoted to the X-ray holographic microscopy whose possibility in principle already has been demonstrated /8,9,10,11/.

An important advantage of holographic microscopy is that the holographic picture contrast (with selection of the optimum reference light) does not depend directly on the sample contrast; it can be highly contrast even for very weak absorption and for a weak-phase shifting samples, as the central part of the passed beam carries only a small fraction of holographic information (of the form of the object under study) and this fraction can often be cancelled in detection. In addition, the hologram enables one to detect also the longitudinal position of the object components at the same time.

An analysis of the requirements to the sources of X-ray radiation for various scheme of X-ray microscopy (including the holographic one ) shows /6/ that the total number of the "effective" quanta from the source is determined only by the spectral brightness of the source  $B_\lambda$

$$\dot{N}_\lambda = B_\lambda \cdot \lambda^2 \cdot \frac{\Delta\lambda}{\lambda} \quad (1)$$

But the necessity of having the monochromatic radiation imposes the limits on the possibilities to use the SR beams from the bending magnets, since "as a rule" the monochromators "spoil" the phase density of the beam of radiation quanta, as the monochromator band pass  $\Delta\lambda/\lambda$  determines an angular spread  $\Delta\theta \sim \Delta\lambda/\lambda$  introduced into the quantum flux. Just this circumstance determines the fact that it is of principal importance for the X-ray holography to use the super bright beams of X-ray radiation from the undulators which do not need the preliminary monochromatization.

As is well known /12,13,14,15,16/ the undulator radiation (UR) has some properties new compared to the SR properties.

The radiation spectral brightness of the N-period undulator is by  $N \cdot N^2$  times higher than that from the bending magnet. In addition, the UR is a quasimonochromatic radiation with  $\Delta\lambda/\lambda \sim 1/N$  and a sharp angular distribution  $\Delta\theta \sim 1/\gamma\sqrt{N}$ . These properties enable one to get the high intensity without substantial deterioration of the UR beam monochromaticity only by selection of the optimal diaphragm size without use of the monochromator. The effective dimensions of the UR source are determined by the electron beam parameters in the storage ring.

One should also note that mainly to development of the X-ray lithography, quite a large number of the X-ray resists appeared recently - the films of various materials (mostly of organic nature) whose etching rate depends on the X-ray radiation dose absorbed in the unit of the X-ray resist volume (the typical value is ranging from  $10 \frac{\text{mJ}}{\text{cm}^3}$  to  $500 \frac{\text{J}}{\text{cm}^3}$ ). The spatial profile obtained on the X-ray resist after etching can be read by an electron microscope. In the soft X-ray wavelength range ( $\lambda \sim 50+100 \text{ \AA}$ ) the X-ray resists have an excellent spatial resolution ( $50+200 \text{ \AA}$ ) and a sensitivity nearing to that of the ideal detector sensitivity when the minimum detected dose corresponds to the absorption of  $1 \pm 10$  quanta per unit sell of the resist volume whose linear dimensions are equal to the resist spatial resolution.

The use of undulators as the sources of X-ray radiation and X-ray resists as the detectors open up new possibilities for the X-ray microholography studies. In the work presented here the experimental study is carried out of the parameters of the UR from the helical undulator, installed in the storage ring VEPP-2M, which are reasoning its use in the holographic schemes.

Without going into the details of theoretical analysis of the UR characteristics performed in a number of papers (see Refs. 12, 16), let us mention some characteristic UR spectral and angular properties. As it is known, the UR n-th harmonic from the individual electron (observed at an angle  $\theta$  with respect to the helical undulator axis) has its wavelength  $\lambda_n$

and the spectral width  $(\Delta\lambda/\lambda)_n$  determined by the following relations:

$$\lambda_n = \frac{\lambda_0}{2n\gamma^2} \cdot (1 + k^2 + \gamma^2\theta^2); \quad \left(\frac{\Delta\lambda}{\lambda}\right)_n = \frac{1}{N \cdot n}; \quad \Delta\theta_{\lambda_n} = \frac{1}{\gamma\sqrt{Nn}} \quad (2)$$

where  $\gamma = E_e/m_e c^2$  is the electron relativistic factor,  $k = 0.0934 \cdot \lambda_0 (\text{cm}) \cdot H_0 (\text{kG})$  - deflection parameter,  $\lambda_0$  - is the helical undulator magnetic period length,  $H_0$  - is the magnetic field amplitude,  $N$  - is the total number of magnetic periods.

For further considerations of the possibilities of the undulator radiation usage in holography let us take a certain example scheme of the Gaborin line axial holography ((an example of the small angular X-ray holography using the SR beam is considered in Ref. 18). The scheme for getting the axial X-ray holographic picture is shown in Fig. 1. The main relations for the resolution capability of this holographic scheme are the following: ( $p \gg q$ )

a) transverse resolution  $\delta_{\perp}$  determined by the radiation source transverse dimensions  $\delta_x, \delta_y$

$$\delta_{\perp} \approx \frac{q}{p} \delta, \quad \delta = \max[\delta_x, \delta_y] \quad (3)$$

b) transverse resolution determined by the screen-detector capability resolution  $\delta_R$

$$\delta_{\perp} \approx \delta_R \quad (4)$$

c) transverse resolution determined by the monochromaticity of radiation  $\Delta\lambda/\lambda$ :

$$\delta_{\perp} \approx \frac{1}{2} \sqrt{q \lambda \cdot \frac{\Delta\lambda}{\lambda}} \quad (5)$$

d) longitudinal resolution determined by the radiation monochromaticity  $\Delta\lambda/\lambda$ :

$$\delta_{\parallel} \approx \frac{q}{4} \cdot \frac{\Delta\lambda}{\lambda} \approx \frac{\delta_{\perp}^2}{\lambda} \quad (6)$$

The organic X-ray resist is used in the scheme as a screen-detector with high resolution. In this case, the holo-

graphic picture exposure time  $t$  with the source spectral brightness  $B_\lambda$  and monochromaticity  $\Delta\lambda/\lambda$  given is determined by the following relations:

$$t \approx \frac{\mathcal{D}}{\mu} \cdot \frac{S}{B_\lambda \lambda^2 \frac{\Delta\lambda}{\lambda}} \approx \frac{\mathcal{D}}{\mu} \cdot \frac{q^2}{B_\lambda \delta_x^2 \frac{\Delta\lambda}{\lambda}} \approx \frac{\mathcal{D}}{\mu} \cdot \frac{p^2}{B_\lambda 2\alpha \delta_x \delta_y \frac{\Delta\lambda}{\lambda}} \quad (7)$$

where  $\mathcal{D}$  is a volume dose ( $\text{J}/\text{cm}^3$ ),  $\mu$  is the resist linear absorption coefficient ( $\text{cm}^{-1}$ ),  $S$  is the hologram area.

Let us get the numerical value for using the undulator as a radiation source installed in the straight section of the storage ring VEPP-2M /17/. This is a helical undulator with a magnetic period length  $\lambda_0 = 2.4$  cm and the total number of periods  $N = 10$ . The magnetic field maximum amplitude on the undulator axis is  $H_0 = 1.3$  kG. Taking into account the electron beam parameters in the place of the undulator location in the storage ring VEPP-2M at an electron energy  $E_e = 0.67$  GeV:  $\delta_{x1} = 0.82$  mrad,  $\delta_y = 0.22$  mrad,  $\delta_x = 0.035$  cm,  $\delta_y = 0.00067$  cm (small coupling  $\alpha = \sqrt{\delta_y \delta_y / \delta_x \delta_x} \ll 1$ ), the undulator spectral brightness  $B_\lambda$  with the field  $H_0 = 1.3$  kG on the UR 1-st harmonic  $\lambda_1 = 79$  Å with a current of 50 mA has the following value

$$B_\lambda = 7.7 \cdot 10^8 \frac{W}{\text{cm}^2 \cdot \text{strad} \cdot \Delta\lambda/\lambda}$$

with the total UR spectral width  $\Delta\lambda/\lambda_1 = 0.20$ . On the other hand, the estimates of the source brightness required for X-ray hologram with resolution of  $\sim 500$  Å and an exposure time of one second give  $B_\lambda \geq 10^7$ .

This evaluation performed does not take into account the additional radiation loss in the sample, substrate, etc. The comparison of this value with those obtained with using in the X-ray holography the SR beams from bending magnets of the storage ring /18/ (taking into account the necessary monochromaticity) emphasizes even more the advantages of the UR usage for solution of such problems.

It is also worth noting the principle possibility to get the X-ray holographic pictures with a spatial resolution of  $\sim 50$  Å using the UR wave length of  $\sim 50$  Å. Diffractional diffusion and the photoelectron free path in the available X-ray resist put the limits on getting higher spatial resolution values ( $\lesssim 50$  Å) /19/.

The absolute measurements of the UR parameters from the helical undulator installed in the storage ring VEPP-2M were carried out at an electron energy  $E_e = 0.39$  GeV and 0.51 GeV within the wavelength range  $100 \div 300$  Å. The magnetic field amplitude on the undulator axis was  $1.0 + 1.1$  kG. This corresponds to the values  $K = 0.224 + 0.247$ . The main goal of these studies was to check up the correspondence of the UR characteristics to the requirements of X-ray holography.

The absolute measurements of the UR spectral angular characteristics have been performed with the grazing incidence monochromator (see Fig. 2) with a gold coated spherical grating  $G$  with a radius of 2 m,  $p = 600$  g/mm.

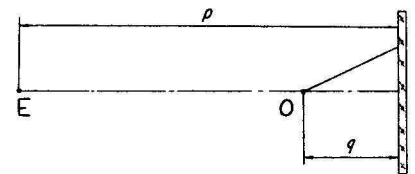


Fig. 1. Axial hologram registration scheme  
 $p$  is a distance between radiation source (E) and the screen (R),  $q$  is a distance between the object (O) and the screen (R)

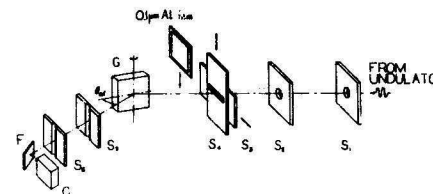


Fig. 2. Scheme of absolute measurements of the UR spectral-angular characteristics

The diffraction angle  $\theta_{diff} \approx 5^\circ$  has been selected by the reasons that at a smaller diffraction angle the scattered background increases and at larger angle the diffraction grating reflection coefficient is substantially decreased in the first order.

The monochromator calibration over the wavelengths has been performed on the Al  $L_{2,3}$  absorption edge by introducing the aluminium foil  $\sim 1000 \text{ \AA}$  thick. The radiation was detected with the channeltron (C) VEU-6 with the CsI(F) photocathode.

The monochromator can be operated without the entrance slit because of the small dimensions of the radiation source  $\delta_x \times \delta_y = 0.25 \times 0.081 \text{ mm}$  (full coupling  $\alpha \sim 1$ ). The collimators  $S_1S_2$  and  $S_5S_6$  are necessary for suppressing the background caused by radiation from the ends of bending magnets. As spectral measurements have shown, the radiation intensity from the bending magnets within the wavelength range  $100 + 300 \text{ \AA}$  is not in excess 5% of the UR intensity at  $\theta = 0$ .

The observation angular aperture  $0.036 \text{ mrad}$  was determined by the entrance diaphragm ( $S_3S_4$ )  $0.2 \times 0.2 \text{ mm}$  and a distance to the source of  $555 \text{ cm}$ . An effective angular dimension of the observation area for the first harmonic was estimated by eq. (2), thus, at  $E_e = 0.51 \text{ GeV}$ ,  $\Delta\theta_{\lambda_1} = 0.32 \text{ mrad}$  and at  $E_e = 0.39 \text{ GeV}$ ,  $\Delta\theta_{\lambda_1} = 0.41 \text{ mrad}$ . As it is seen, an angular aperture after diaphragm is ten times smaller than an angular size of the first harmonic. The small size of the diaphragm enabled studying directly the UR spectral-angular density.

The electron beam angular spread for VEPP-2M are  $\delta_{x1} = 0.628 \text{ mrad}$ ,  $\delta_{y1} = 0.167 \text{ mrad}$  at an energy  $E_e = 0.51 \text{ GeV}$ . The calculated curve for the UR spectral-angular density (taking into account the electron angular spread and the beam transverse dimensions) is drawn in Fig. 3. The UR 1-st harmonic wavelength is  $\lambda_1 = 132.9 \text{ \AA}$ , the spectral width is  $(\Delta\lambda/\lambda)_1 = 0.144$ , an absolute spectral-angular density is  $9.3 \cdot 10^{11} \frac{\text{phot}}{\text{s} \cdot \text{mA} \cdot \text{mrad}^2} \cdot 1\% \text{ b.w.}$  that is by 1.43 times higher compared to that observed (Fig. 4), which is  $6.5 \cdot 10^{11}$ .

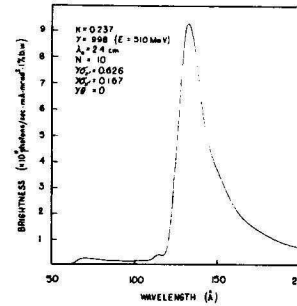


Fig. 3. Calculated UR spectrum  
 $E_e = 0.51 \text{ GeV}$  ( $\gamma = 998$ ),  
 $k = 0.237$ ,  $\theta = 0$

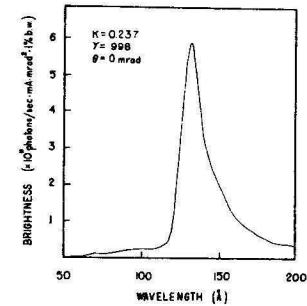


Fig. 4. Observed UR spectrum  
 $E_e = 0.51 \text{ GeV}$  ( $\gamma = 998$ ),  
 $k = 0.237$ ,  $\theta = 0$

The SR from the bending magnet of the storage ring VEPP-2M at  $E_e = 0.51 \text{ GeV}$  has  $3.1 \cdot 10^{10}$  at the same wavelength. This is by 21 times lower than that observed UR. As seen from the measured spectrum, the UR second harmonic is not observed. This fact is connected with the small reflection coefficient of the diffraction grating in the corresponding wavelength range. In addition, in this case, the spectral-angular density of the UR 2-nd harmonic is 50 times lower than that for the 1-st harmonic. For simultaneous observation of the 1-st and 2-nd UR harmonics the measurements have been carried out of an electron energy  $E_e = 0.39 \text{ GeV}$ . In this case, the wavelengths for the UR both harmonics are in spectral window of the used monochromator:  $100 + 300 \text{ \AA}$ .

The UR spectra were obtained at  $E_e = 0.39 \text{ GeV}$  ( $\gamma = 763$ )  $k = 0.224$ , for  $\gamma\theta = 0, 0.15, 0.25, 0.35$  (Fig. 5). The spectra are not normalized over the grating reflection coefficient, therefore the harmonic ratio on the spectrum is not correct. Fig. 6 shows the wavelength for both UR harmonics as a function of the observation angle  $\theta$ . The electron angular spread and the UR spectral width  $(\Delta\lambda/\lambda)_n = 1/N_n$  lead to the displacement of the wavelength for the first and second UR harmonics compared to that given by relation (2) and also lead to the violation of the dependence on  $\theta^2$  in the region of the observation

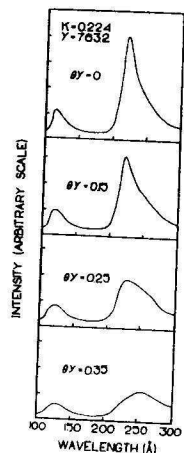


Fig. 5. Observed UR spectra  $E_e = 0.39$  GeV ( $\gamma = 763$ ),  $k = 0.224$ ,  $\theta = 0, 0.15, 0.25, 0.35$  or  $\theta = 0, 0.20, 0.33, 0.46$  Mrad

small angles ( $\theta \lesssim \delta_{x'}, \delta_{y'}$ ). The difference between the observed and calculated angular dependencies caused by an inaccuracy in angular calibration of  $\theta$  values. The same reason causes the difference in the UR spectral-angular density dependency on the observation angle values. The curves obtained are normalized over the calculated value at  $\theta = 0$ .

The UR spectral-angular characteristic measurements do not supply the direct information on the effective transverse size of radiation source which is important in setting up the holographic experiments. According to the electron

beam size in the storage ring VEPP-2M the helical undulator radiation should have sufficiently high level of spatial coherence. For an electron energy  $E = 0.51$  GeV at the transverse dimensions of the electron beam  $d_x = 2.36 \cdot \delta_x = 0.059$  cm,  $d_y = 2.36 \cdot \delta_y = 0.019$  cm the coherence region size at a distance from the source  $P = 520$  cm are the following  $C_x = \lambda_2 P / d_x = 110 \mu\text{m}$ ,  $C_y = \lambda_2 P / d_y = 360 \mu\text{m}$  at the wavelength of UR  $\lambda_2 = 130$  Å. The experiments on the real spatial coherence observation of the VEPP-2M undulator radiation have been performed by studying the interference pictures from two small ( $\approx 6 \mu\text{m}$ ) holes in  $2 \mu\text{m}$  thick Si-membrane coated with  $0.3 \mu\text{m}$  Au and increasing the difference between the holes until disappearance of the interference bands. The optical scheme of the experiments is given in Fig. 8. The negative X-ray resist ELN-200 ( $D \sim 10 \text{ J/cm}^2$ ,  $\mu \sim 10^5 \text{ cm}^{-1}$ ) ( $0.2 \mu\text{m}$  thick film is put on the silicon substrate) is used as the detector-screen. Its exposure time, according to the spectral-angular measurements described above, is estimated as  $I \cdot t \approx 10 \text{ A} \cdot \text{s}$ . Fig. 9 shows the interference pictures for some distances between the holes in the study of both

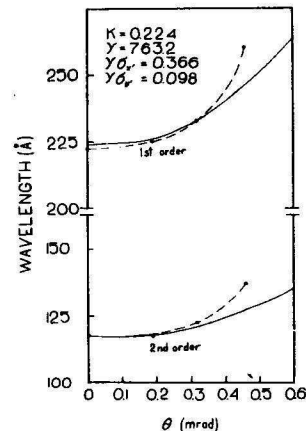


Fig. 6. Angular dependence of the UR wavelengths on 1-st ( $n=1$ ) and 2-nd ( $n=2$ ) harmonics  
 ---- observed curve (see Fig.5);  
 ——— calculated curve ( $\gamma \delta_{x'} = 0.366$ ,  $\gamma \delta_{y'} = 0.098$ ).

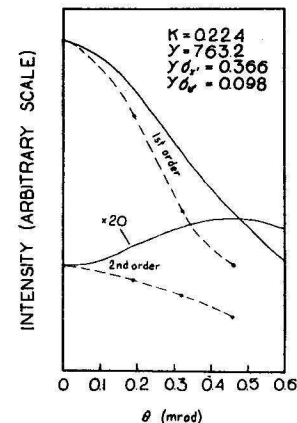


Fig. 7. Angular dependence of the UR spectral-angular densities of the 1-st ( $n=1$ ) and 2-nd ( $n=2$ ) harmonics  
 ---- observed curve (see Fig.5);  
 ——— calculated curve ( $\gamma \delta_{x'} = 0.366$ ,  $\gamma \delta_{y'} = 0.098$ ).

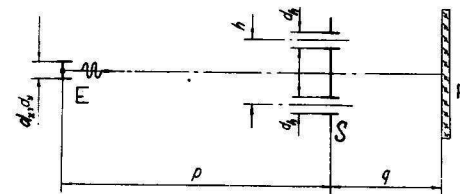


Fig. 8. The spatial coherence registration scheme  $d_x, d_y$  - transverse dimensions of the radiation source  $y(E)$  ( $d_x = 0.059$  cm,  $d_y = 0.019$  cm),  $p$  - a distance between the source (E) and absorption screen (S) ( $p=520$  cm);  $h, d_h$  - a distance between holes and their diameters in the screen (S) ( $d_h \approx 6 \mu\text{m}$ );  $q$  - a distance between the screen (S) and detector-screen (R) ( $q=31$  cm)

the vertical (a) and horizontal (b) spatial coherence.

According to the estimates obtained, the UR satisfies the requirements for its use in the X-ray holographic microscopy. The absolute measurements of the UR characteristics from



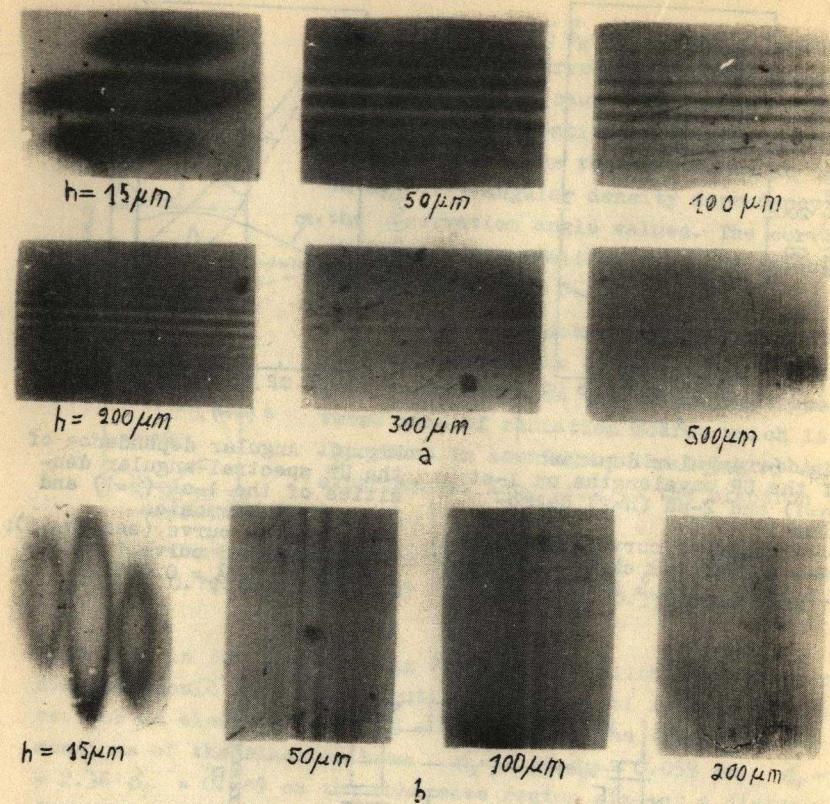


Fig. 9. Interference pictures obtained for different distances between the holes  $h$  during measurements of vertical (a) and horizontal (b) UR spatial coherence. Typical exposure  $I \cdot t \sim 20 \text{A} \cdot \text{s}$ , where  $I$  - storage ring current.

the helical undulator installed in the storage ring VEPP-2M are in a good agreement with the calculation estimates of the UR spectral-angular density which took into account the electron beam parameters in the storage ring. The experiments on the UR demonstrate that the use of UR is perspective for the X-ray holography, and show that the estimates of the spatial coherence area are correct. In conclusion, the authors wish to acknowledge Dr. P.M.Ivanov for the help in the spectral-angular measurements and Dr. V.V.Chesnokov's group for the preparing of the Si-membranes and the X-ray resists.

### References

1. R.Feder et al.: Science, 197, p. 259, 1977.
2. P.Horowitz, J.A.Howell: Science, 178, p. 608, 1972.
3. B.Nieman et al.: Appl. Opt., 15, p. 1882, 1976.
4. B.Nieman et al.: NIM, p. 367, 1983.
5. R.P.Haelbich et al. A Scanning Ultrasoft X-ray Microscope with Large Aperture Reflection Optics for Use with Synchrotron Radiation: Preprint DESY SR-79/190, 1979.
6. A.M.Kondratenko, A.N.Skrinsky: Avtometriya, 2, p. 3, 1977.
7. G.N.Kulipanov, A.N.Skrinsky, UPhN, 122, Iss. 3, p. 369, 1977.
8. S.Kikuta et al.: Opt. Commun., 5, 86, 1972.
9. O.J.Sasoccio: J. Opt. Soc. Am., 57, p. 966, 1967.
10. S.Hoki et al.: Jpn. J. Appl. Phys., 13, p. 1385, 1974.
11. V.V.Aristov et al.: Opt. Commun., 34, N 3, p. 332, 1980.
12. D.F.Alferov et al.: Part. Acceler., 9, p. 223, 1970.
13. A.N.Didenko et al.: Sov. Phys., 49, p. 973, 1979.
14. A.S.Artamonov et al.: NIM, 177, p. 239, 1980.
15. H.Maezawa et al.: NIM, 208, 151, 1983.
16. D.F.Alferov, Yu.A.Bashmakov: "Spectral-angular characteristics of radiation of the beam of relativistic charged particle in undulator", Preprint, FIAN SSSR, N77, 1983.
17. G.Ya.Kezerashvili et al.: Proc. All Union Conf. on Utilis. of SR (SR-82), Novosibirsk, 1982.
18. A.M.Kondratenko, A.N.Skrinsky: "The use of radiation from the storage rings in X-ray holography of microobjects", Preprint INP 75-102, Novosibirsk, 1975.
19. E.S.Gluskin et al.: NIM, 208, p. 393, 1983.

Е.С.Глускин, П.П.Ильинский, Г.Я.Кезерашвили,  
Г.Н.Кулипанов, В.Ф.Пиндурин, А.Н.Скринский,  
А.С.Соколов

ИССЛЕДОВАНИЕ ИЗЛУЧЕНИЯ ИЗ СПИРАЛЬНОГО ОНДУЛЯТОРА,  
УСТАНОВЛЕННОГО НА НАКОПИТЕЛЕ ВЭП-2М, КАК ИСТОЧ-  
НИКА ДЛЯ РЕНТГЕНОВСКОЙ МИКРОСКОПИИ И ГОЛОГРАФИИ

Препринт  
№ 83-145

Работа поступила - 22 декабря 1983 г.

---

Ответственный за выпуск - С.Г.Попов  
Подписано к печати 30.XII-1983 г. МН 03516  
Формат бумаги 60x90 1/16 Усл.0,8 печ.л., 0,6 учетно-изд.л.  
Тираж 290 экз. Бесплатно. Заказ № 145.

---

Ротапринт ИЯФ СО АН СССР, г.Новосибирск, 90